Measurement of two-photon production of the χ_{c2}

J. Dominick,[1] S. Sanghera,[1] V. Shelkov,[1] T. Skwarnicki,[1] R. Stroynowski,[1] I. Volobouev,[1] P. Zadorozhny,[1] M. Artuso,[2] D. He,[2] M. Goldberg,[2] N. Horwitz,[2] R. Kennett,[2] G. C. Moneti,[2] F. Muheim,[2] Y. Mukhin,[2] S. Playfer,[2] Y. Rozen,[2] S. Stone,[2] M. Thulasidas,[2] G. Vasseur,[2] G. Zhu,[2] J. Bartelt,[3] S. E. Csorna,[3] Z. Egyed,[3] V. Jain,[3] P. Sheldon,[3] D. S. Akerib,[4] B. Barish,[4] M. Chadha,[4] S. Chan,[4] D. F. Cowen,[4] G. Eigen,[4] J. S. Miller,[4] C. O'Grady,[4] J. Urheim,[4] A. J. Weinstein,[4] D. Acosta,[5] M. Athanas,[5] G. Masek,[5] H. Paar,[5] M. Sivertz,[5] A. Bean,[6] J. Gronberg,[6] R. Kutschke,[6] S. Menary,[6] R. J. Morrison,[6] S. Nakanishi,[6] H. N. Nelson,[6] T. K. Nelson,[6] J. D. Richman,[6] A. Ryd,[6] H. Tajima,[6] D. Schmidt,[6] D. Sperka,[6] M. S. Witherell,[6] M. Procario,[7] S. Yang,[7] R. Balest,[8] K. Cho,[8] M. Daoudi,[8] W. T. Ford,[8] D. R. Johnson,[8] K. Lingel,[8] M. Lohner,[8] P. Rankin,[8] J. G. Smith,[8] J. P. Alexander,[9] C. Bebek,[9] K. Berkelman,[9] D. Besson,[9] T. E. Browder,[9] D. G. Cassel,[9] H. A. Cho,[9] D. M. Coffman,[9] P. S. Drell,[9] R. Ehrlich,[9] R. S. Galik,[9] M. Garcia-Sciveres,[9] B. Geiser,[9] B. Gittelman,[9] S. W. Gray,[9] D. L. Hartill,[9] B. K. Heltsley,[9] C. D. Jones,[9] S. L. Jones,[9] J. Kandaswamy,[9] N. Katayama,[9] P. C. Kim,[9] D. L. Kreinick,[9] G. S. Ludwig,[9] J. Masui,[9] J. Mevissen,[9] N. B. Mistry,[9] C. R. Ng,[9] E. Nordberg,[9] M. Ogg,[9,*] J. R. Patterson,[9] D. Peterson,[9] D. Riley,[9] S. Salman,[9] M. Sapper,[9] H. Worden,[9] F. Würthwein,[9] P. Avery,[10] A. Freyberger,[10] J. Rodriguez,[10] R. Stephens,[10] J. Yelton,[10] D. Cinabro,[11] S. Henderson,[11] K. Kinoshita,[11] T. Liu,[11] M. Saulnier,[11] F. Shen,[11] R. Wilson,[11] H. Yamamoto,[11] B. Ong,[12] M. Selen,[12] A. J. Sadoff,[13] R. Ammar,[14] S. Ball,[14] P. Baringer,[14] D. Coppage,[14] N. Copty,[14] R. Davis,[14] N. Hancock,[14] M. Kelly,[14] N. Kwak,[14] H. Lam,[14] Y. Kubota,[15] M. Lattery,[15] J. K. Nelson,[15] S. Patton,[15] D. Perticone,[15] R. Poling,[15] V. Savinov,[15] S. Schrenk,[15] R. Wang,[15] M. S. Alam,[16] I. J. Kim,[16] B. Nemati,[16] J. J. O'Neill,[16] H. Severini,[16] C. R. Sun,[16] M. M. Zoeller,[16] G. Crawford,[17] M. Daubenmeir,[17] R. Fulton,[17] D. Fujino,[17] K. K. Gan,[17] K. Honscheid,[17] H. Kagan,[17] R. Kass,[17] J. Lee,[17] R. Malchow,[17] F. Morrow,[17] Y. Skovpen,[17,†] M. Sung,[17] C. White,[17] J. Whitmore,[17] P. Wilson,[17] F. Butler,[18] X. Fu,[18] G. Kalbfleisch,[18] M. Lambrecht,[18] W. R. Ross,[18] P. Skubic,[18] J. Snow,[18] P. L. Wang,[18] M. Wood,[18] D. Bortoletto,[19] D. N. Brown,[19] J. Fast,[19] R. L. McIlwain,[19] T. Miao,[19] D. H. Miller,[19] M. Modesitt,[19] S. F. Schaffner,[19] E. I. Shibata,[19] I. P. J. Shipsey,[19] P. N. Wang,[19] M. Battle,[20] J. Ernst,[20] H. Kroha,[20] S. Roberts,[20] K. Sparks,[20] E. H. Thorndike,[20] and C. H. Wang[20]

(CLEO Collaboration)

[1] *Southern Methodist University, Dallas, Texas 75275*
[2] *Syracuse University, Syracuse, New York 13244*
[3] *Vanderbilt University, Nashville, Tennessee 37235*
[4] *California Institute of Technology, Pasadena, California 91125*
[5] *University of California, San Diego, La Jolla, California 92093*
[6] *University of California, Santa Barbara, Calfornia 93106*
[7] *Carnegie-Mellon University, Pittsburgh, Pennsylvania 15213*
[8] *University of Colorado, Boulder, Colorado 80309-0390*
[9] *Cornell University, Ithaca, New York 14853*
[10] *University of Florida, Gainesville, Florida 32611*
[11] *Harvard University, Cambridge, Massachusetts 02138*
[12] *University of Illinois, Champaign-Urbana, Illinois 61801*
[13] *Ithaca College, Ithaca, New York 14850*
[14] *University of Kansas, Lawrence, Kansas 66045*
[15] *University of Minnesota, Minneapolis, Minnesota 55455*
[16] *State University of New York at Albany, Albany, New York 12222*
[17] *Ohio State University, Columbus, Ohio 43210*
[18] *University of Oklahoma, Norman, Oklahoma 73019*
[19] *Purdue University, West Lafayette, Indiana 47907*
[20] *University of Rochester, Rochester, New York 14627*

(Received 4 October 1993; revised manuscript received 22 February 1994)

The CLEO II detector is used to search for the production of χ_{c2} states in two-photon interactions. We use the signature $\chi_{c2} \to \gamma J/\psi \to \gamma l^+ l^-$ with $l = e, \mu$. Using 1.49 fb^{-1} of data taken with beam energies near 5.29 GeV, the two-photon width of the χ_{c2} is determined to be $\Gamma(\chi_{c2} \to \gamma\gamma) = 1.08 \pm 0.30(\text{stat}) \pm 0.26(\text{syst})$ keV, in agreement with predictions from perturbative QCD.

PACS number(s): 14.40.Gx, 13.20.Gd, 13.40.Hq, 13.65.+i

*Permanent address: Carleton University, Ottawa, Canada K1S 5B6.
†Permanent address: INP, Novosibirsk, Russia.

I. INTRODUCTION

The discoveries of the ψ and Υ families of resonances have prompted many theoretical and experimental investigations into heavy quark systems. Although heavy quark potential models have proven valuable in the study of S-wave states, difficulties in treating the wave function of P-wave states have made theoretical progress more difficult. One intriguing approach makes use of a combination of nonperturbative lattice QCD methods and perturbative QCD calculations [1] to calculate the relative rate for the doubly radiative decays of ^3P_J states. In the charm sector this is given approximately by

$$\frac{\Gamma(\chi_{c2} \to \gamma\gamma)}{\Gamma(\chi_{c2} \to gg)} = \frac{8}{8}\frac{\alpha^2}{\alpha_s^2} . \quad (1)$$

The decay of the χ_{c2} to light hadrons does not proceed exclusively through two gluons. Instead the quarks may radiate a third gluon, transforming the original $q\bar{q}$ pair from a color-singlet P-wave to a color-octet S-wave state. Heavy quarks do not easily radiate a gluon, and so the three-gluon decay width is suppressed by a factor of order v^2 where v is the typical heavy quark velocity. However, the angular momentum barrier suppresses the annihilation of a $q\bar{q}$ P-wave state into two gluons by a similar factor of v^2. Therefore the decay of the χ_{c2} into light hadrons proceeds via comparable amounts of two-gluon and three-gluon intermediate states.

In order to extract the two-gluon width of the χ_{c2} from the total hadronic decay width, the color-octet contribution must be subtracted. This color-octet contribution is independent of J, so should be equal to the total hadronic decay width of the χ_{c1}, for which the color-singlet decay to two gluons is forbidden by angular momentum conservation. In this way the two-gluon decay width of the χ_{c2} can be determined from the hadronic decay widths of the χ_{c2} and χ_{c1} by

$$\Gamma(\chi_{c2} \to gg) = \Gamma(\chi_{c2} \to \text{hadrons}) - \Gamma(\chi_{c1} \to \text{hadrons}) . \quad (2)$$

Using the value of $\Gamma(\chi_{cJ} \to \text{hadrons})$ calculated by subtracting the radiative width $\Gamma(\chi_{cJ} \to \gamma J/\psi)$ [2] from the total width [3] it is possible to obtain a prediction for the two-photon branching fraction of the χ_{c2}. This branching ratio is predicted [1] to be $B(\chi_{c2} \to \gamma\gamma) = (4.1 \pm 1.1 \pm 1.5) \times 10^{-4}$, or equivalently $\Gamma_{\gamma\gamma} = 0.82 \pm 0.23 \pm 0.30$ keV where the first error is from uncertainties in the experimental inputs, and the second error is an estimate of the theoretical uncertainty [4].

This paper reports a measurement of the cross section for the production of χ_{c2} in the two-photon interaction $e^+e^- \to e^+e^-\chi_{c2}$. The χ_{c2} is observed through its decay to J/ψ and a photon, with the J/ψ identified in its decay to e^+e^- or $\mu^+\mu^-$. The theoretical cross section scales linearly with the two-photon width of the χ_{c2}, so it is possible to extract the two photon width by comparing the calculated cross section with the observed cross section.

Section II gives a description of the detector, particle identification, and event selection criteria. The Monte Carlo simulation is explained in detail in Sec. III. Section IV gives the results of the cross-section measurement and the two-photon width, and a discussion of the uncertainties in the analysis. Results are summarized in Sec. V.

II. SELECTION OF χ_{c2} CANDIDATE EVENTS

The CLEO II detector [5] consists of three concentric proportional wire drift chambers surrounded by a time-of-flight scintillation system and an electromagnetic calorimeter consisting of 7800 cesium iodide crystals. The crystals are used for identifying electrons and measuring the energy of photons. The transverse momentum resolution of the tracking chambers is given by $\sigma_p^2/p^2 = (0.0015)^2p^2 + (0.0050)^2$, and the energy resolution of the calorimeter is parametrized by $\sigma_E/E = 0.0035/E^{0.75} + 0.019 - 0.001E$ in the barrel, and $\sigma_E/E = 0.0026/E + 0.025$ in the end cap, where both p and E are measured in GeV. Surrounding the calorimeter is a 1.5 T superconducting coil. Outside the coil are three layers of iron interleaved with three layers of muon detection chambers.

A major experimental difficulty of this measurement is triggering the readout of the detector reliably while still discriminating against the very common beam-gas and beam-wall events. A multilevel trigger is provided using information from the tracking chambers, scintillators, and calorimeter crystals. Two types of triggers are selected: one for γe^+e^- final states and the other for $\gamma\mu^+\mu^-$ final states. For electron pair final states there must be at least one cluster of more than 0.5 GeV in the calorimeter, two reconstructed tracks in the tracking chambers, and two separated hits in the scintillators. The trigger for the muon pair final states requires at least two separated calorimeter signals consistent with minimum ionizing tracks, two reconstructed tracks, and two separated hits in the scintillators. For events with tracks within the geometric acceptance of the detector, these trigger requirements have an efficiency of 0.94 ± 0.01 for electron pair events and 0.84 ± 0.01 for muon pair events, while rejecting most high rate backgrounds.

Events with two oppositely charged tracks are selected for further analysis. Both tracks are required to pass track quality criteria and originate near the interaction point. This largely rejects cosmic ray, beam-gas, and beam-wall events.

Candidates for the decays $\chi_{c2} \to \gamma e^+e^-$ and $\chi_{c2} \to \gamma\mu^+\mu^-$ must have one and only one photon candidate with energy greater than 0.3 GeV. The photon produced in the decay of the χ_{c2} typically deposits 0.46 GeV in the calorimeter, making a cut at 0.3 GeV very efficient for χ_{c2} decays. For photon identification a cluster of energy in the calorimeter is required to be more than 30 cm from the projected impact point of any charged track. The photon must be detected at an angle more than 18° from the beam axis ($\cos\theta_\gamma < 0.95$), in order to avoid a region where tracking efficiency is poor and spurious photons are plentiful. Photon candidates below 0.3 GeV are not

considered.

In searching for $ee\gamma$ or $\mu\mu\gamma$ final states, most backgrounds come from events with real e^+e^- or $\mu^+\mu^-$ pairs and real photons. Particle misidentification does not contribute significantly to the background; therefore lepton identification requirements are kept loose. For electron identification, the ratio of the energy deposited in the calorimeter ($E_{\rm cal}$) to the momentum as measured by the tracking chambers (p) is used. If the ratio satisfies $0.85 < E_{\rm cal}/p < 1.10$ for both tracks in the event, it is classified as an electron pair event. This criterion gives an efficiency of 0.81 ± 0.01 as determined from Monte Carlo (MC) simulation of the $E_{\rm cal}/p$ distribution. The background in the muon channel is smaller than in the electron channel; therefore, the criterion for muon identification can be looser. If at least one of the two charged tracks has an associated track in the muon chambers, the event is assumed to contain a muon pair. This gives an efficiency of 0.97 for identifying a muon pair event.

The total momentum of the event is defined as the vector sum of the momenta of the two leptons and the candidate photon. The component of the total momentum perpendicular to the beam is called the total transverse momentum, P_T. Events with $P_T < 0.5$ GeV/c are selected. This rejects events of the type $e^+e^- \to \tau^+\tau^-$ where the τ pair gives rise to a lepton pair, or a misidentified pion and any number of soft photons. Events of this type will usually have a large P_T imbalance due to the missing energy carried by the neutrinos.

The total visible energy of the event is defined as the scalar sum of the momenta of the charged tracks and the candidate photon. It does not include neutral energy clusters of less than 0.3 GeV. The dominant background in this analysis is from e^+e^- interactions following initial state radiation. Since the energy of the χ_{c2} is typically less than half the center of mass energy, we require the total visible energy of the event to be less than 5.4 GeV. This has an efficiency of 0.99 for χ_{c2} events, and removes virtually all of the background due to initial state radiation.

The QED process $e^+e^- \to \gamma_i\gamma_f e^+e^-$, where the photon from initial state radiation, γ_i, is at small angles and is not detected, is another source of background. If the initial state photon is detected, the event will fail the total visible energy cut above. The photon from final state radiation or bremsstrahlung in the beam pipe, γ_f, will tend to point in the same direction as the track, producing a large excess of events at $\cos\theta_{\gamma e^\pm} = 1$. To suppress this background, the angle between the candidate photon direction and the direction of each track at the interaction point is required to be greater than 15° ($\cos\theta_{\gamma e^\pm} < 0.965$). This requirement is not necessary for the muon pair events.

Finally, the invariant mass of the two tracks must be consistent with the mass of the J/ψ. The mass resolution of the J/ψ can be determined by studying the invariant mass of the two charged tracks for events which pass all other χ_{c2} selection criteria, shown in Fig. 1. When fit by a Gaussian, the width is $\sigma = 12$ MeV/c^2, in agreement with the width expected from a MC model. A cut at $m_{J/\psi} \pm 30$ MeV/c^2 is chosen to optimize the significance

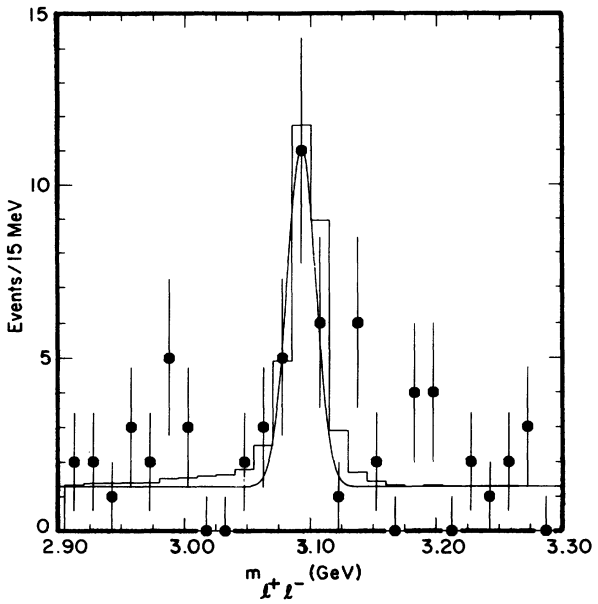

FIG. 1. Two-particle reconstructed mass for events which have a $l^+l^-\gamma$ effective mass consistent with the χ_{c2}. Data are shown as points, MC as a histogram. The fit is to a Gaussian plus a flat background.

of the MC signal relative to the background observed in the data.

III. MONTE CARLO SIMULATION

A two-photon MC simulation based on the formalism of Budnev [6] is used to generate χ_{c2} final states. The cross section can be expressed as a sum of four two-photon cross-section terms and two interference intensities, each depending upon the different polarizations of the photons. The interference terms vanish when integrated over azimuth. Of the remaining four cross-section terms, three involve at least one longitudinally polarized photon. These contribute only if at least one photon is off mass shell. Since we require that the scattered e^+ and e^- are not observed, both photons are predominantly near the mass shell. Thus only the cross-section term involving two transversely polarized photons contributes, and the total cross section is then related to the two-photon cross section by

$$d\sigma_{e^+e^-\to e^+e^-\chi_{c2}} = d\mathcal{L}^{TT}_{\gamma\gamma}(W^2)\sigma^{TT}_{\gamma\gamma\to\chi_{c2}} , \qquad (3)$$

where $\mathcal{L}^{TT}_{\gamma\gamma}$ is the $\gamma\gamma$ luminosity function and W is the two-photon invariant mass.

Transverse photons can produce χ_{c2} particles with helicity 0 or 2 only. The helicity 0 state has zero two-photon partial width [7] in the nonrelativistic approximation. For this reason, only the σ^{TT} term representing the cross section for χ_{c2} production of helicity 2 is significant. σ^{TT} is determined [8] by

$$\sigma^{TT}_{\gamma\gamma\to\chi_{c2}} = \frac{F^2_{TT2}}{4\sqrt{X}}\frac{m^2}{W}\frac{\Gamma}{(W^2-m^2)^2+\Gamma^2m^2} , \qquad (4)$$

where

$$X = \frac{1}{4}(W^2 - q_1^2 - q_2^2)^2 - q_1^2 q_2^2 \ . \tag{5}$$

Γ and m are the total width and mass of the χ_{c2} and $q_i^2 < 0$ is the square of the momentum transfer to each of the two photons. F_{TT2} is the form factor for the helicity 2 state of the χ_{c2}.

To model the q^2 dependence [8], we use the J/ψ form factor

$$F_{TT2}^2(q_1^2, q_2^2) = (2J+1)16\pi m\Gamma_{\gamma\gamma} \times \frac{1}{(1 - q_1^2/m_{J/\phi}^2)^2} \frac{1}{(1 - q_2^2/m_{J/\psi}^2)^2} \ . \tag{6}$$

$J = 2$ is the spin of the χ_{c2} and $\Gamma_{\gamma\gamma}$ is the two-photon width of the χ_{c2} state.

The resonant production process is characterized by four independent variables. The MC generates the azimuthal angle between the two scattered electrons (ϕ), the two polar angles of the scattered electrons (θ_1, θ_2), and the energy of one of the radiated photons (ω_1). The energy of the second radiated photon (ω_2) is calculated using the mass of the χ_{c2} state. For the line shape of the χ_{c2}, we use a Breit-Wigner function with a total width of $\Gamma = 2$ MeV [2,3].

In order to describe the angular distribution of the final state particles in the decay $\chi_{c2} \to J/\psi\gamma \to l^+l^-\gamma$, it is necessary to know the decay amplitudes for each helicity. The production amplitude is significant for helicity 2 only, measured with respect to the χ_{c2} direction. The decay amplitudes for helicity 2, 1, and 0, measured with respect to the $J/\psi - \gamma$ axis in the χ_{c2} rest frame, are all significant. In terms of these helicity decay amplitudes, the distribution of the final state particles is

$$\begin{aligned} f(\theta^*, \theta', \phi') = {} & \tfrac{1}{8}A_2^2(1+\cos^2\theta')(1+6\cos^2\theta^*+\cos^4\theta^*) + \tfrac{1}{2}A_1^2(1-\cos^2\theta')(1-\cos^4\theta^*) \\ & + \tfrac{3}{4}A_0^2(1+\cos^2\theta')(1-2\cos^2\theta^*+\cos^4\theta^*) + \frac{\sqrt{2}}{2}A_2A_1(\sin 2\theta'\cos\phi')(\sin\theta^*+3\sin\theta^*\cos^2\theta^*) \\ & + \frac{\sqrt{6}}{4}A_2A_0(\sin^2\theta'\cos 2\phi')(1-\cos^4\theta^*) - \sqrt{3}A_1A_0(\sin 2\theta'\cos\phi')(\sin\theta^*\cos\theta^* - \sin\theta^*\cos^3\theta^*) \ . \end{aligned} \tag{7}$$

θ^* is the angle of the photon direction relative to the photon-photon collision axis in the rest frame of the χ_{c2}, while θ' and ϕ' define the positron direction in the J/ψ rest frame relative to the J/ψ direction of motion. The decay amplitudes for helicity 2, 1, and 0 have been measured [9] as $A_2 = 0.848^{+0.042}_{-0.050}, A_1 = 0.485^{+0.066}_{-0.073}, A_0 = 0.213^{+0.033}_{-0.022}$. If the decay is treated as a pure electric dipole ($E1$) transition, the values of the decay helicity amplitudes would be $A_2 = 0.775, A_1 = 0.548, A_0 = 0.316$. The MC events are generated isotropically in $\cos\theta^*, \cos\theta'$, and ϕ', and the events passing all cuts are weighted by the approximate angular distribution.

The CLEO II detector has excellent J/ψ mass resolution allowing very tight mass cuts to be made. However, this also requires that the J/ψ line shape be correctly modeled in the MC for an accurate measurement of the efficiency. Final state radiation in the decay $J/\psi \to e^+e^-$ is very significant, resulting in a 31% reduction in efficiency when compared to MC decays without final state radiation. This effect cannot be ignored even in the muon pair final state. This effect causes the overall efficiency for e^+e^- final states to be somewhat smaller than for $\mu^+\mu^-$ final states.

The simulation of the transport of the final state photon and leptons through the CLEO II detector is performed by a GEANT-based MC routine which makes use of EGS for electromagnetic showers. The events generated with this MC are then processed by the same analysis program used on the data.

IV. EXPERIMENTAL RESULTS

In order to measure the cross section for $e^+e^- \to e^+e^-\chi_{c2}$, the mass difference spectrum is studied. The mass difference is defined here as $\Delta_m = m_{l^+l^-\gamma} - m_{l^+l^-} - 0.459$ GeV/c^2, where the expected mass difference has been subtracted. The mass difference is used because the $l^+l^-\gamma$ mass spectrum and the l^+l^- spectrum are both broadened by final state radiation from the leptons. The difference, Δ_m, is much less susceptible to this broadening. Figure 2 shows the $m_{l^+l^-\gamma}$ distribution for all events passing the event selection criteria listed in Sec. II. When fit to a Gaussian it has $\sigma = 18$ MeV. The mass difference distribution, shown in Fig. 3, has $\sigma = 12$ MeV.

It is evident that the mass difference distribution has a peak near zero and some slowly varying background. In order to estimate the background, a subtraction is made using events in the sidebands of the J/ψ mass plot. The signal band about the mass of the J/ψ is ± 30 MeV/c^2, from 3.067 GeV/c^2 to 3.127 GeV/c^2. The low and high sidebands are defined as the regions of the lepton pair mass distribution 2.7 GeV/c^2 to 3.0 GeV/c^2 and 3.2 GeV/c^2, to 3.5 GeV/c^2, respectively. The mass difference plots are made for the events in the sideband regions as well, and these distributions are scaled by the ratio of the interval widths, 0.1. The scaled mass difference distribution of the sidebands is shown in Fig. 4 along with the signal. The sidebands are a good match

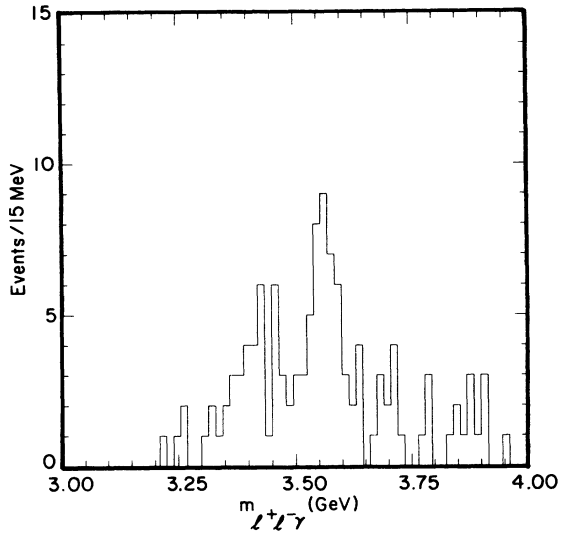

FIG. 2. Three-particle reconstructed mass, $m_{l^+l^-\gamma}$.

to the background over much of the plot [10]. In order to reduce the impact of statistical fluctuations in the sideband mass difference distribution, the distribution is fit using a function of the form $f(q) = Aq^B e^{-Cq}$ where $q = (\Delta m - D)$. The four parameters A, B, C, and D are determined using a maximum likelihood fit.

Detector acceptance and efficiency of the analysis cuts are estimated with a MC simulation. The signal is fit using the shape of the MC distribution. The background is estimated by fixing the parameters B, C, and D at the values obtained in a fit to the scaled sidebands. The

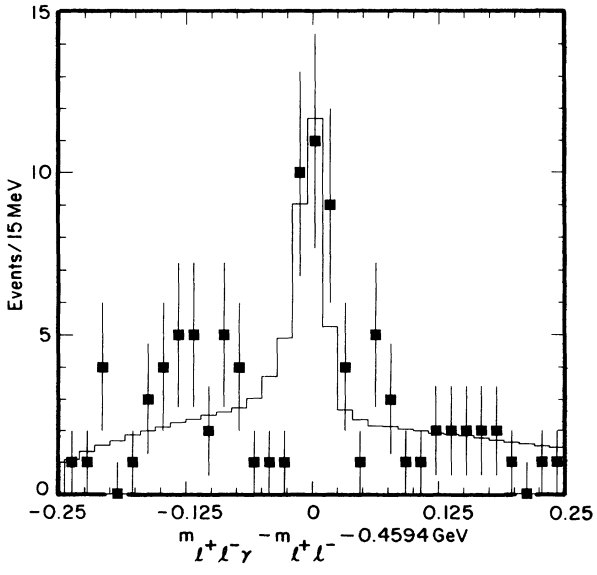

FIG. 3. The mass difference between the $l^+l^-\gamma$ effective mass and l^+l^- effective mass, $m_{l^+l^-\gamma} - m_{l^+l^-} - 0.459\ \mathrm{GeV}/c^2$. The PDG mass difference between the χ_{c2} and J/ψ has been subtracted so that the events of interest should peak at 0. The histogram is the sum of the scaled MC signal shape and the scaled background shape obtained from J/ψ mass sideband data.

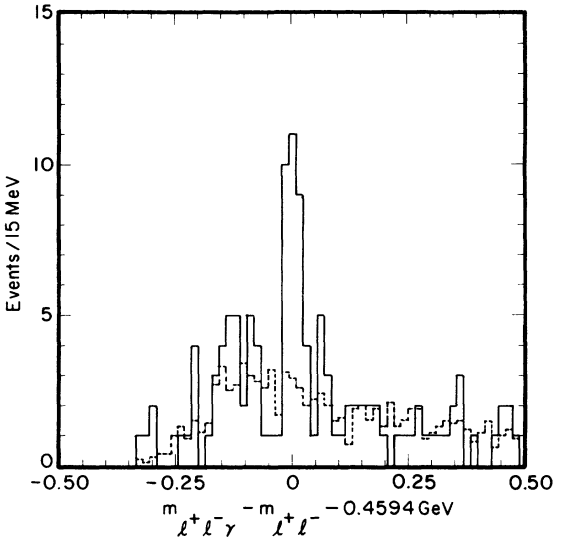

FIG. 4. The mass difference between the $l^+l^-\gamma$ effective mass and l^+l^- effective mass, $m_{l^+l^-\gamma} - m_{l^+l^-} - 0.459\ \mathrm{GeV}/c^2$. The solid histogram is from events with a dilepton mass consistent with a J/ψ, while the dashed histogram is from the J/ψ sidebands. The sideband histogram has been scaled by a factor of 0.1 to account for the ratio of interval widths.

normalization parameter A of the background function is allowed to vary, as is the normalization of the MC signal shape. This two-parameter fit, shown in Fig. 3, yields $N_{ee\gamma+\mu\mu\gamma} = 25.4 \pm 6.9$ events.

The product of the acceptance and efficiency for observing a final state $ee\gamma$ or $\mu\mu\gamma$, $\epsilon_{ee\gamma+\mu\mu\gamma}$, is determined from the Monte Carlo simulation:

$$\epsilon_{ee\gamma+\mu\mu\gamma} = \frac{N_{ee\gamma}^{\mathrm{found}} + N_{\mu\mu\gamma}^{\mathrm{found}}}{N_{ee\gamma}^{\mathrm{generated}} + N_{\mu\mu\gamma}^{\mathrm{generated}}}\ , \tag{8}$$

where the number of $\mu\mu\gamma$ events generated is equal to the number of $ee\gamma$ events generated times the ratio of branching fractions $B(J/\psi \to \mu\mu)/B(J/\psi \to ee)$. This gives an efficiency of $\epsilon_{ee\gamma+\mu\mu\gamma} = 0.187 \pm 0.003$, where the error listed is statistical only.

The cross section is calculated from

$$\sigma(e^+e^- \to e^+e^-\chi_{c2}) = \frac{1}{L}\frac{1}{B_{J/\psi\gamma}}\frac{1}{B_{\mu\mu}+B_{ee}}\frac{N_{ee\gamma+\mu\mu\gamma}}{\epsilon_{ee\gamma+\mu\mu\gamma}} \tag{9}$$

by taking account of the leptonic branching fraction of the $J/\psi (B_{ee} = 0.0627 \pm 0.0020$ for $J/\psi \to ee$ and $B_{\mu\mu} = 0.0597 \pm 0.0025$ for $J/\psi \to \mu\mu)$, the radiative branching fraction of the $\chi_{c2} (B_{J/\psi\gamma} = 0.135 \pm 0.011)$, and the integrated luminosity ($L = 1.49 \pm 0.02\ \mathrm{fb}^{-1}$). The result of $N_{ee\gamma+\mu\mu\gamma} = 25.4 \pm 6.9$ events yields a measured cross section of $\sigma(e^+e^- \to e^+e^-\chi_{c2}) = 5.5 \pm 1.6 \pm 1.3$ pb, where the first uncertainty is statistical and the second is systematic. This result uses the helicity decay amplitudes as reported in Ref. [9] (see Sec. III). Assuming that the decay of the χ_{c2} is a pure electric dipole transition reduces the calculated cross section by 3%.

The systematic uncertainties due to inaccurate simula-

TABLE I. Determinations of $\Gamma_{\gamma\gamma}(\chi_{c2})$.

Experiment [12]	$\Gamma_{\gamma\gamma}(\chi_{c2})$ (keV)
Crystal Ball [13]	2.8 ± 2.0
R704 [14]	$2.9^{+1.3}_{-1.0}$
CLEO 1.5 [15]	< 1.0 (95% C.L.)
TPC/2γ [16]	3.4 ± 1.7
E760 [17]	0.321 ± 0.078
This experiment	1.08 ± 0.30
Theory [1]	0.82 ± 0.23

tion of the data are estimated by observing the change in the measured cross section as selection criteria are varied. Most MC distributions agree well with the data when account is taken of the background. The largest contributions to the systematic uncertainty come from the cut on the photon angular distribution and the transverse momentum cut, with minor contributions coming from the visible energy cut and the J/ψ mass cut. The cut on the cosine of the photon angle was varied from 0.5 to 1.0 with a resultant change in the cross section of $\pm 15\%$. Varying the transverse momentum cut between 0.1 GeV/c and 1.0 GeV/c contributed 14% to the uncertainty in the cross section. Changing the visible energy cut in the range 4–6 GeV gave results that contributed 7% to the systematic uncertainty while changing the J/ψ mass acceptance window in the range from ± 10 MeV/c^2 to ± 100 MeV/c^2 made an 8% contribution to the uncertainty in the calculated cross section.

Another source of uncertainty is the form factor used. We have studied the effect of using a ρ form factor, a J/ψ form factor, and no q^2 dependence at all in Eq. (6). Using no q^2 dependence gives a long tail at large values of $-q^2$, the J/ψ form factor gives a somewhat smaller tail, and the ρ form factor gives almost no tail to the q^2 distribution. The cross section for χ_{c2} production is sensitive to the form factor used, dropping by 24% for ρ. Since this experiment has the largest acceptance for events with q^2 very near 0, there is a compensating increase in the efficiency which very nearly cancels the change in the cross section. The uncertainty in the measured cross section depends upon the product of the MC cross section and the MC detection efficiency, and is nearly independent of the form factor selected. The observed variation in the measured cross section is $\pm 5\%$.

These effects have been combined in quadrature to give the final 24% systematic uncertainty. The small sample size precludes any significant reduction in the determination of the systematic uncertainty.

The two-photon width can be extracted from the measured cross section by scaling by the ratio of these values used in the MC simulation:

$$\Gamma_{\gamma\gamma} = \Gamma^{\rm MC}_{\gamma\gamma}\left(\frac{\sigma}{\sigma_{\rm MC}}\right) . \qquad (10)$$

There are additional systematic uncertainties in the derivation of the two-photon width from the cross section. We assume that the χ_{c2} is produced predominantly in the helicity 2 state. The helicity 0 state has zero two-photon partial width in the nonrelativistic approximation, while in other models it is predicted to be between 2% and 5% of the helicity 2 state. Thus, the assumption that the helicity 2 production amplitude is dominant for the χ_{c2} state introduces an additional theoretical uncertainty of $^{+5}_{-0}\%$.

Longitudinally polarized photons require nonzero values of q_i^2. Large values of $-q_i^2$ are relatively rare, and the ratio of the σ_{TL} term to the σ_{TT2} term is estimated [11] to be much less than 1%.

These effects, added in quadrature with the previous systematic error, give a systematic uncertainty on the two-photon width of 24%. With these additional systematic uncertainties, the two-photon width of the χ_{c2} is determined to be $\Gamma_{\gamma\gamma} = 1.08 \pm 0.30 \pm 0.26$ keV, corresponding to a branching fraction of $B(\chi_{c2} \to \gamma\gamma) = (5.4 \pm 1.6 \pm 1.3) \times 10^{-4}$. This can be compared to the theoretical prediction of $\Gamma_{\gamma\gamma} = 0.82 \pm 0.23 \pm 0.30$ keV and $B(\chi_{c2} \to \gamma\gamma) = (4.1 \pm 1.1 \pm 1.5) \times 10^{-4}$. Table I compares this result to other experimental determinations of the two-photon width of the χ_{c2}. Many of these experiments share similar systematic and theoretical uncertainties [12] so only statistical uncertainties are listed.

Following the treatment of Ref. [1], the result for $\Gamma_{\gamma\gamma}$ can be combined with Γ_{gg} to derive a value for α_s using Eqs. (1) and (2). $\Gamma(\chi_{cJ} \to \text{hadrons})$ is derived by subtracting the radiative width $\Gamma(\chi_{cJ} \to \gamma J/\psi)$ [2] from the total width [3] to obtain $\Gamma(\chi_{c2} \to \text{hadrons}) = 1.73 \pm 0.18$ MeV and $\Gamma(\chi_{c1} \to \text{hadrons}) = 0.64 \pm 0.15$ MeV. Using the assumption that the color-octet decay width of the χ_{c2} is the same as that of the χ_{c1}, the two-gluon width of the χ_{c2} is determined to be $\Gamma(\chi_{c2} \to gg) = 1.09 \pm 0.23$ MeV. This yields a value of $\alpha_s(m_c) = 0.219 \pm 0.078 \pm 0.053 \pm 0.085$, in reasonable agreement with expectations. The first uncertainty is statistical, the second is systematic, and the third is the contribution from theoretical uncertainties.

V. CONCLUSIONS

In summary, we have measured the cross section for the production of the χ_{c2} in the process $e^+e^- \to e^+e^-\chi_{c2}$ to be $\sigma(e^+e^- \to e^+e^-\chi_{c2}) = 5.5 \pm 1.6 \pm 1.3$ pb. This implies a two-photon width for the χ_{c2} of $\Gamma_{\gamma\gamma} = 1.08 \pm 0.30 \pm 0.26$ keV. These results were obtained using J/ψ form factors in the two-photon propagators, and the assumption that only transversely polarized photons are significant in the production of the χ_{c2} state.

ACKNOWLEDGMENTS

We gratefully acknowledge the effort of the CESR staff in providing us with excellent luminosity and running conditions. We thank G. P. Lepage for his patient discussion of QCD as it applies to this analysis. J. P. A. and P. S. D. thank the PYI program of the NSF, I.P.J.S. thanks the YI program of the NSF, G. E. thanks the Heisenberg Foundation, K. K. G. and A. J. W. thank the SSC program of TNRLC, K. K. G., H. N. N., J. D. R., and H. Y. thank the OJI program of DOE, and P. R. thanks the A. P. Sloan Foundation for support. This work was supported by the National Science Foundation and the U. S. Department of Energy.

[1] G. T. Bodwin, E. Braaten, and G. P. Lepage, Phys. Rev. D **46**, 1914 (1992).

[2] Particle Data Group (PDG), K. Hikasa *et al.*, Phys. Rev. D **45**, S1 (1992).

[3] Hikasa *et al.* [2]. The measurements of total widths are dominated by the results of the E760 Collaboration, T. A. Armstrong *et al.*, Nucl. Phys. **B373**, 35 (1992), which differ very slightly from the world average.

[4] These values are obtained from Ref. [1] where the authors used $\alpha_s(m_c) = 0.25$.

[5] Y. Kubota *et al.*, Nucl. Instrum. Methods Phys. Res. Sect. A **320**, 66 (1992).

[6] V. M. Budnev *et al.*, Phys. Rep. **15C**, 181 (1975).

[7] Z. P. Li, F. E. Close, and T. Barnes, Phys. Rev. D **43**, 2161 (1991).

[8] An excellent review of this material can be found in the article by M. Poppe, Int. J. Mod. Phys. A **1**, 545 (1986).

[9] E760 Collaboration, T. A. Armstrong *et al.*, Phys. Rev. D **48**, 3037 (1993).

[10] The data contain real J/ψ decays which will not be accounted for by a sideband subtraction. By combining a real J/ψ with accidental photons which have an energy distribution that peaks sharply at the 0.3 GeV cutoff it is possible to produce an apparent peak in the $m_{l^+l^-\gamma}$ distribution near $m_{J/\psi} + E_{\rm cutoff}$. This artifact, which can be seen in both the mass plot (Fig. 2) and the mass difference plot (Fig. 4), shifts with the cutoff energy. There is, as yet, no unambiguous evidence for the observation of two photon production of χ_{c0} states decaying via $\gamma J/\psi$ in our current data set.

[11] This estimate has been derived from the forms given in Ref. [8], p. 609.

[12] Differences in assumptions used in determining the two-photon width make detailed comparisons difficult. It should be noted that the leptonic branching ratios of the J/ψ, as listed in the PDG, changed by $\approx 13\%$ since several of these measurements were made. The published value for the total width of the χ_{c2} has also been revised recently. In addition, the angular distribution of the final state photons has been treated in a variety of ways in the different analyses. No corrections have been applied.

[13] Crystal Ball Collaboration, R. A. Lee *et al.*, Stanford Report No. SLAC 282, 1985 (unpublished).

[14] R704 Collaboration, C. Baglin *et al.*, Phys. Lett B **187**, 191 (1987).

[15] CLEO Collaboration, W.-Y. Chen *et al.*, Phys. Lett. B **243**, 169 (1990).

[16] TPC/2γ Collaboration, D. A. Bauer *et al.*, Phys. Lett. B **302**, 345 (1993).

[17] E760 Collaboration, T. A. Armstrong *et al.*, Phys. Rev. Lett. **70**, 2988 (1993).